

# We are IntechOpen, the world's leading publisher of Open Access books Built by scientists, for scientists

5,200

Open access books available

128,000

International authors and editors

150M

Downloads

Our authors are among the

154

Countries delivered to

TOP 1%

most cited scientists

12.2%

Contributors from top 500 universities



WEB OF SCIENCE™

Selection of our books indexed in the Book Citation Index  
in Web of Science™ Core Collection (BKCI)

Interested in publishing with us?  
Contact [book.department@intechopen.com](mailto:book.department@intechopen.com)

Numbers displayed above are based on latest data collected.  
For more information visit [www.intechopen.com](http://www.intechopen.com)



# Solar Radiation in Buildings, Transfer and Simulation Procedures

Jose Maria Cabeza Lainez  
University of Seville  
Spain

## 1. Introduction

Solar radiation is the only renewable energy source readily available at every building in the world. Whilst urban regulations and meteorological or geographical factors often impede proper ventilation, to design a building without at least a view of the surroundings is tantamount to making plans for a prison or a tomb, and no culture would accept that as a permanent residence. Thus, the necessary connections with the environment are provided by apertures through which radiation is admitted.

Since antiquity, a multitude of researchers and scientists have striven to find the magnitude of solar radiation incident on a horizontal surface at the earth's crust. A few of them have found adroit correlations between horizontal and vertical irradiation. These seem acceptable for the analysis of building facades since direct measurements are in many cases not feasible due to obstructions, interferences with ground reflection or simply because of economic constraints.

However, it is still surprising how few scholars are familiar with the distribution of such radiation inside the chambers, precisely where it should be used. To be sure, if one wants to transfer a certain amount of energy to human beings, the task needs to be accomplished piecemeal, or the consequences could be devastating as, unfortunately, everybody knows.

In the ensuing chapter, the author intends to explain the fundamentals of radiative energy transfer, a discontinued branch of geometric optics that colligates time, space and architecture in a single operation. The author would also try to ensure that every person is able to reproduce his experiments at home by virtue of computer simulation and analysis.

## 2. Radiative transfer between spherical surfaces

Let us start by discussing radiative exchanges in simple volumes. The sphere is a volume enclosed by only one surface and with some restrictions it is used both in engineering and architecture. If the inner surface of the sphere emits under Lambertian diffusion, the total fraction of energy reaching the same surface will be one hundred percent, that is: the unity.

In mathematical terms this is expressed as:

$$F_{11}=1 \quad (1)$$

The fraction of energy leaving surface 1 and arriving at surface 1, is one. The former gives rise to a new algebra defined by:

$$F_{11} + F_{12} + \dots + F_{1n} = 1 \quad (2)$$

In a closed volume, by the principle of energy conservation, and disregarding transmission losses, radiant energy emitted by surface  $i$  is necessarily distributed in its entirety among the surrounding surfaces. As an example, in a cube, where all faces are equal, the fraction of energy leaving from an internal source to any of the other five is  $1/5=0.2$ .

As the radiant flux is originated in a given surface and bears only nominal relationship with the medium in which the phenomena take place, the distribution of such flux will be a function of the dimensions of the surfaces involved. Thus we could anticipate a second and final property for our algebra (Lambert, 1764).

$$A_i \cdot F_{ij} = A_j \cdot F_{ji} \quad (3)$$

Where  $A_i$  is the area of surface  $i$  and  $F_{ij}$  is the fraction of energy that leaves  $i$  and reaches  $j$ .

Returning to the sphere, it is easy to see that although interior radiation may occur, unless we are able to pierce the surface by means of some kind of section, interaction with the environment remains negligible. Any planar section of the sphere will produce a spherical cap with a circular base that works as an aperture. (See Figure 1).

The size of the aperture is determined by the height of the cap,  $h$ . Beginning with the case of a hemisphere, the said height coincides with the radius of the sphere  $R=a=h$ .

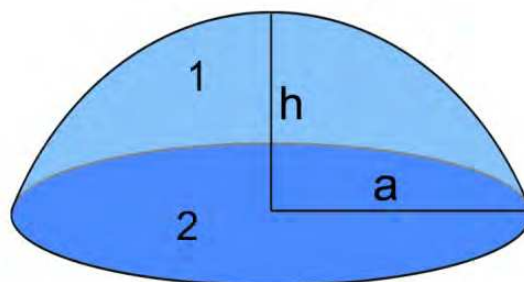


Fig. 1. Surfaces generated by a spherical cap

In this situation, there are two surfaces involved in the radiation problem. Let us apply the former algebra to them.

If for the whole sphere  $F_{11} = 1$ , taking into account the dependence on area of radiative transfer, it is assumed that for the hemisphere  $F_{11} = 1/2 = 0.5$ , and the demonstration will be given later in the text.

By equation (2) the former also implies that  $F_{12} = 0.5$ . Thus, half of the flux of the hemisphere is distributed over itself and the other half is ceded to the circular base that serves as an aperture of the sphere.

In accordance with this reasoning, for a cap whose area equals one third (1/3) of the whole surface,  $F_{11}=1/3$  and  $F_{12}=2/3$  and so on.

When the respective areas of surfaces 1 and 2 are introduced, the fraction of energy that leaves 1 and arrives at 2 equates the area-ratio of such potential sources. In this way, equation 3 is proved if we remember that, for the spherical cap,  $F_{21}$  has to be one. The circle is a planar figure and gives one hundred percent of its energy to the surrounding cap.

$$F_{12} = \frac{a^2}{a^2+h^2} \tag{4}$$

It is inferred that  $F_{11} = 1- F_{12}$ , and its value would be,

$$F_{11} = \frac{h^2}{a^2+h^2} \tag{5}$$

Substituting into equation 5, the trigonometric relation for the radius of the sphere,  $R$ ,

$$a^2 + h^2 = 2 * R * h \tag{6}$$

We obtain an extremely important and beautiful expression,

$$F_{11} = \frac{h}{2*R} \tag{7}$$

Thus, by simple logic, and with hardly any calculus, the author has solved for the first time in this field one of the most complex integral equations of environmental science (Eq. 8).

$$\Phi_{1-2} = E_{b1} \int_{A_1} \int_{A_2} \cos\theta_1 * \cos\theta_2 * \frac{dA_1*dA_2}{\pi*r^2} = E_{b1} * \pi * a^2 \tag{8}$$

Where  $\Phi_{1-2}$  is the radiative flux exchange between the surfaces considered, and  $E_{b1}$  is the radiant energy emitted by surface 1. The relative ease of the solution is partly due to the fact that the quantities termed  $\cos\theta_i$ , which represent the cosines of the angles between the line going from the center of surface 1 to the center of surface 2 and their respective normals, are simpler to find in this case as the said normals always pass through the center of the sphere.

It is convenient to use the former results in an ample variety of ways.

For instance, if the aforementioned division of the sphere is performed by means of two planar sections, like in a quarter of sphere (see Figure 2), the solutions are still valid, in the sense that the quarter of a sphere is giving itself one fourth of its emissive power  $F_{33}=1/4$ .

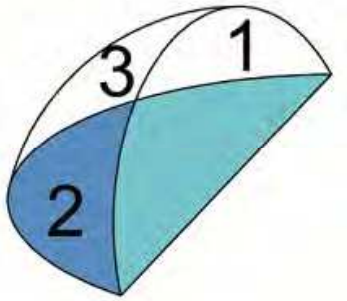


Fig. 2. Surfaces generated by a quarter of a sphere

As we already found, the two semicircles receive in total 3/4 of the flux, but provided that they are of equal area, each one of them receives  $3/8 = F_{32} = F_{31}$ .

Thus, equation 2 is fulfilled.  
By equation 3, the so-called principle of reciprocity,  $F_{13} = F_{23} = 2 \cdot \pi \cdot R^2 / \pi \cdot R^2 \cdot F_{31} = 3/4$   
And this implies that  $F_{12} = F_{21} = 1/4$   
A second complex integral equation has been solved by the author without calculus.

In a similar manner, adjusting the fragment of sphere which the problem may demand, the radiative exchange between semicircles with a common edge, forming any angle from 0 to 180 degrees, can be found. The above example is valid for 90 degrees.

The author has been the first to propose the following equation, previously unheard of in the literature, to obtain the energy balance between the said semicircles, where x represents the value of the internal angle (Fig. 3),

$$F_{12} = 1 - \frac{x}{90} + \frac{x^2}{32400}$$

(9)

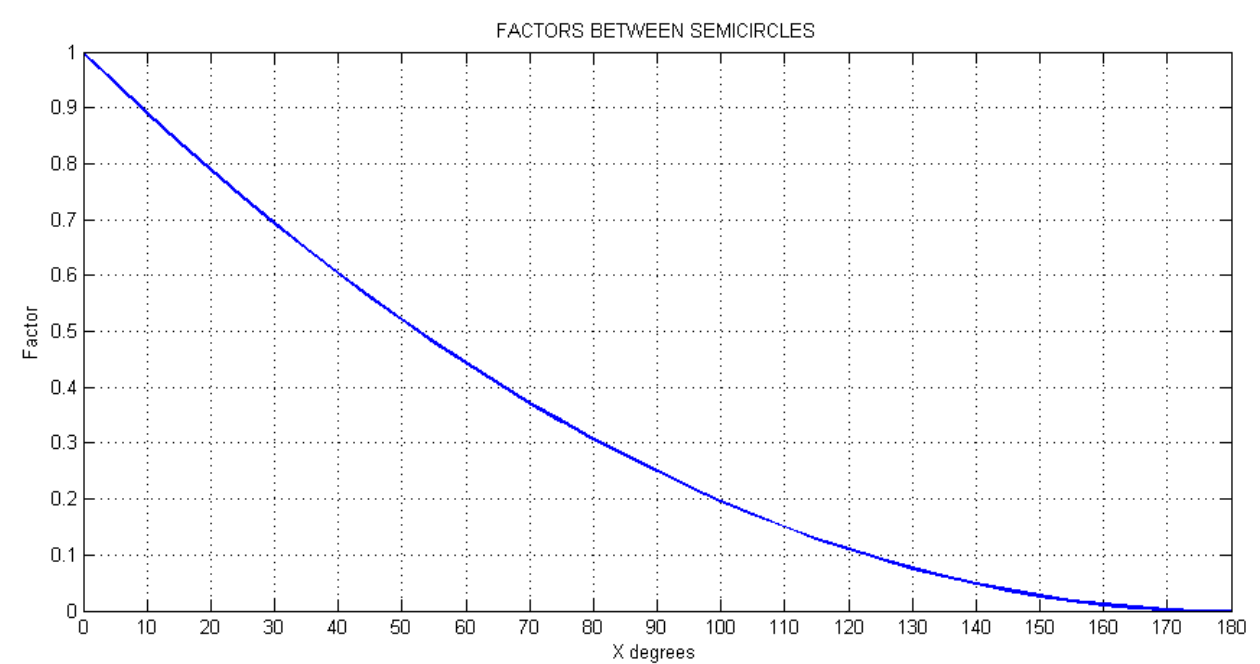


Fig. 3. Radiative exchanges between two semicircles with a common edge and forming an internal angle  $x$

So far so good. The former expression solves a whole set of integral equations and anybody can understand how the radiant flux is transferred from circular or semicircular apertures to the interior of the sphere as a total fraction. However, it is often useful to examine this transfer in more detail, i.e. point by point.

2.1 Radiative transfer between spherical surfaces and points

Referring again to the sphere in respect with the canonical equation 8; if you look at figure 4, it is easy to find the relationship between  $r$ ,  $\cos\theta$  and the radius of the sphere  $R$ .

$$\phi_{1-2} = \frac{E_{b1}}{4 \cdot \pi \cdot R^2} \int_{A_1} \int_{A_2} dA_1 \cdot dA_2 \tag{10}$$

$4 \cdot \pi \cdot R^2$  is obviously the area of the sphere. Thus, the radiative flux transfer is dependent on the size of the surfaces but not on their position on the sphere and for a given area it is also a constant.

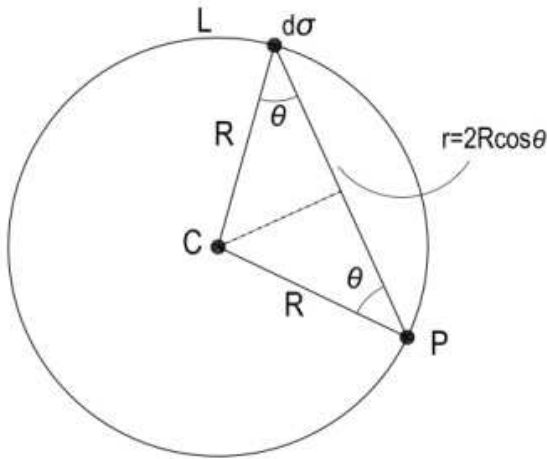


Fig. 4. Differential surfaces in the sphere used to find the radiative exchange

Those properties are unique to the spherical surface and also crucial for our discussion. At this point, if we return to the spherical cap described in figure 1, there the flux from the cap to the circle was defined. However, assuming this circle to be virtual or, in other words, transparent to radiation, what remains behind is simply the opposite cap of the sphere, now called surface 2 for convenience.

The fraction of energy emitted from 1 to the new surface 2 is the same as in equation 4, but the energy received by surface 2 is  $F_{21}$ , and we can obtain it from the theorem of reciprocity finding the ratio between the respective areas.

The area of surface 2 is,

$$A_2 = \pi \cdot (a^2 + (2 \cdot R - h)^2) \tag{11}$$

$$F_{21} = \frac{\pi \cdot a^2}{\pi \cdot (a^2 + (2 \cdot R - h)^2)} \tag{12}$$

And from equation 6,

$$a^2 + h^2 = 2 \cdot R \cdot h \tag{13}$$

$$F_{21} = \frac{a^2 \cdot h^2}{a^4 + 2 \cdot h^4 - 2 \cdot h^4 + 3 \cdot a^2 \cdot h^2 - 2 \cdot a^2 \cdot h^2} \tag{14}$$

$$F_{21} = \frac{a^2 \cdot h^2}{a^2 \cdot (a^2 + h^2)} = \frac{h^2}{a^2 + h^2} = \frac{h}{2 \cdot R} \tag{15}$$

This equates the fraction defined as  $F_{11}$  for the spherical cap. Let us see it depicted in a different graph (Figure 5).

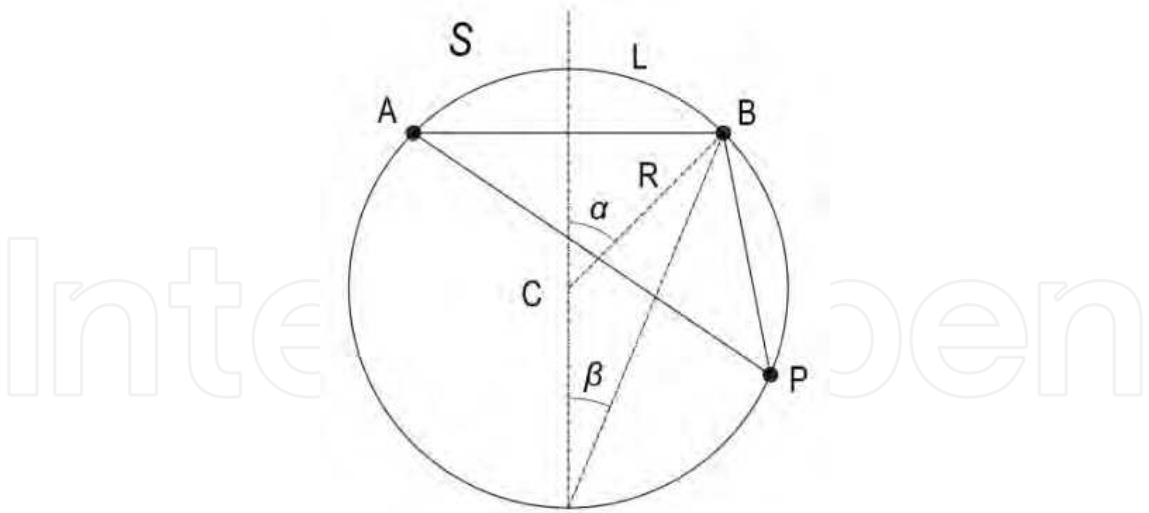


Fig. 5. Cap and sphere where the radiative exchange takes place

In figure 5, the cap  $S$  goes from  $A$  to  $B$  and its area is  $\pi \cdot 2 \cdot R \cdot h$ , as mentioned above (Eq. 6). Dividing the former by the total area of the sphere according to equation 10, the result is as shown in Equations 7 and 15. That is, the energy received at any point of the interior sphere wall outside the spherical cap  $S$  is constant,  $h/2 \cdot R$ . This is often expressed as  $1/2 \cdot (1 - \cos \alpha)$  or  $1/2 \cdot (1 - \cos 2\beta)$ .

With the former property we can replace the cap source by its enclosed circle  $AB$ .

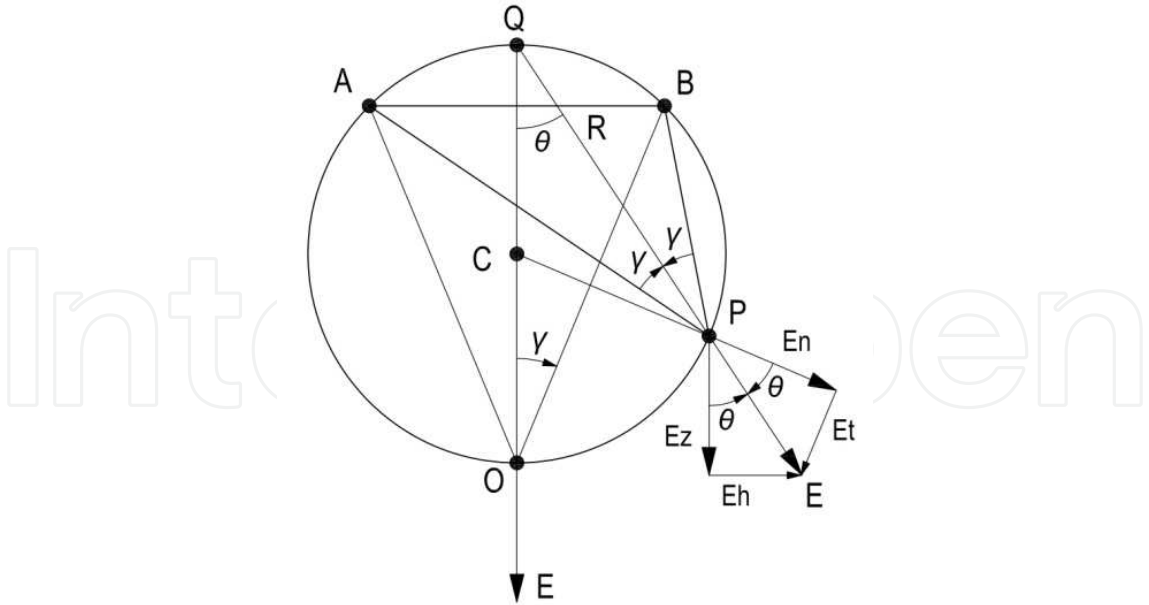


Fig. 6. The radiation vector in a sphere

Radiant energy due to the spherical cap or the said circle, in a direction normal to the interior of the sphere, is constant but it is mandatory not to forget that radiation is in truth a vector, meaning that its projection on different planes may present diverse values.

Finding the radiation vector that originates in the cap source poses no particular problem (See Figure 6). For reasons of symmetry, its centre has to be at point Q, following the well-known principle of the circumference by virtue of which, equal arcs subtend equal angles<sup>1</sup>.

The extreme of the vector lies at the point under study. If the direction of the vector is known, it only remains to calculate its modulus. Using trigonometric properties, as the normal  $E_N$  is constant, this implies that the vertical component  $E_Z$  equates the normal for the value of direction angle  $\theta$  is a half of the angle subtended by the arc OP from the centre of the sphere, being P the point under study and O the horizontal projection of the centre.

The last step to determine the modulus of the vector is to project its vertical component  $h/(2 \cdot R)$  onto the horizontal plan, multiplying by the tangent of  $\theta$ .

The fact that the vertical component is constant has led to the construction of useful graphs in which horizontal radiation  $E_Z$  at a given point is obtained as a function of the radius of the cap's base and the distance from the circle's centre to the point considered (See figures 7 and 8).

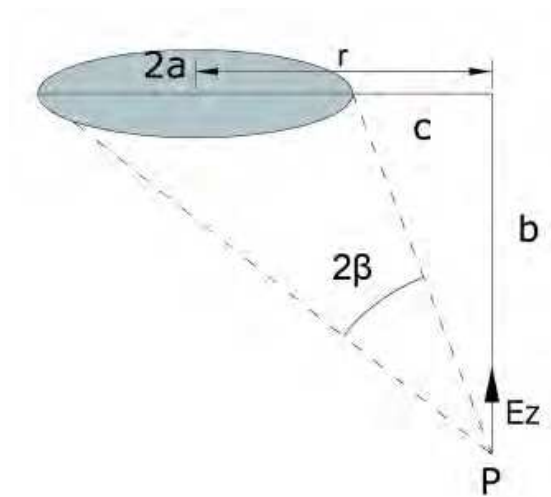


Fig. 7. Perpendicular component of the radiation vector under a disk

If the said quantities are known, the coordinate component  $E_H$ , which is constant only for the same height over the horizontal in the sphere, in other words, by parallels, can be found employing the circumference's properties.

$$R^2 = a^2 + \left(\frac{b^2+r^2-a^2}{2b}\right)^2 \tag{16}$$

$$h = R - \sqrt{R^2 - a^2} \tag{17}$$

And the vertical distance from the origin of the radiation vector to the point considered is, evidently,

$$d = b + h \tag{18}$$

<sup>1</sup> Both MacAllister and Sumpner failed to see this point and located the origin of the vector at the centre of the enclosed circle, though this error may be relevant for sizeable sources.



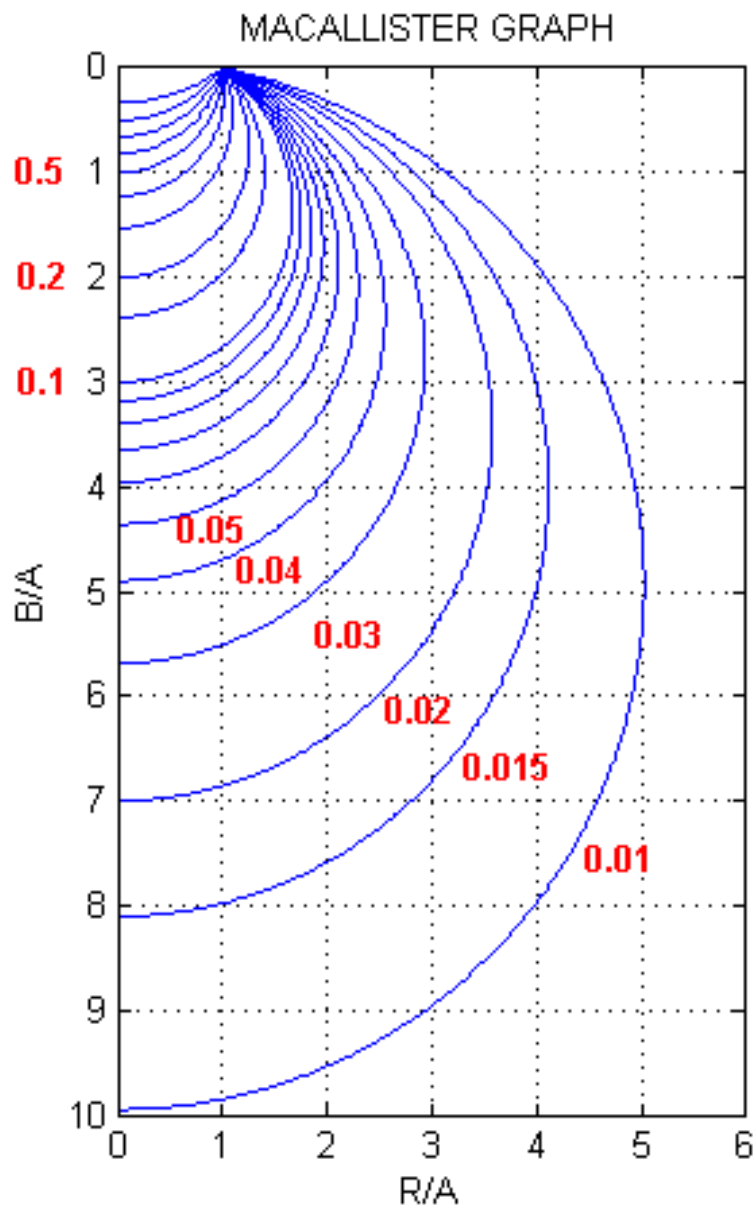


Fig. 8. The MacAllister graph for finding the vertical component of radiation, using only the magnitudes on figure 7 and without need for calculation

To obtain the vectorial field of radiation around a spherical cap source or its equivalent disk (the final aim of radiative transfer and simulation for such common geometry) is tantamount to finding a set of virtual spheres which contains both the source and each one of the points considered in the reticule that represents the field. From this set we extract the components and consequently the radiation vector at each point of the domain analysed.

The author has created original software that simulates the aforementioned fields for planes, spheres and cylinders at every possible inclination angle in spherical coordinates,  $\theta$  or  $\varphi$ ; some results are presented in figures 9 and 10.

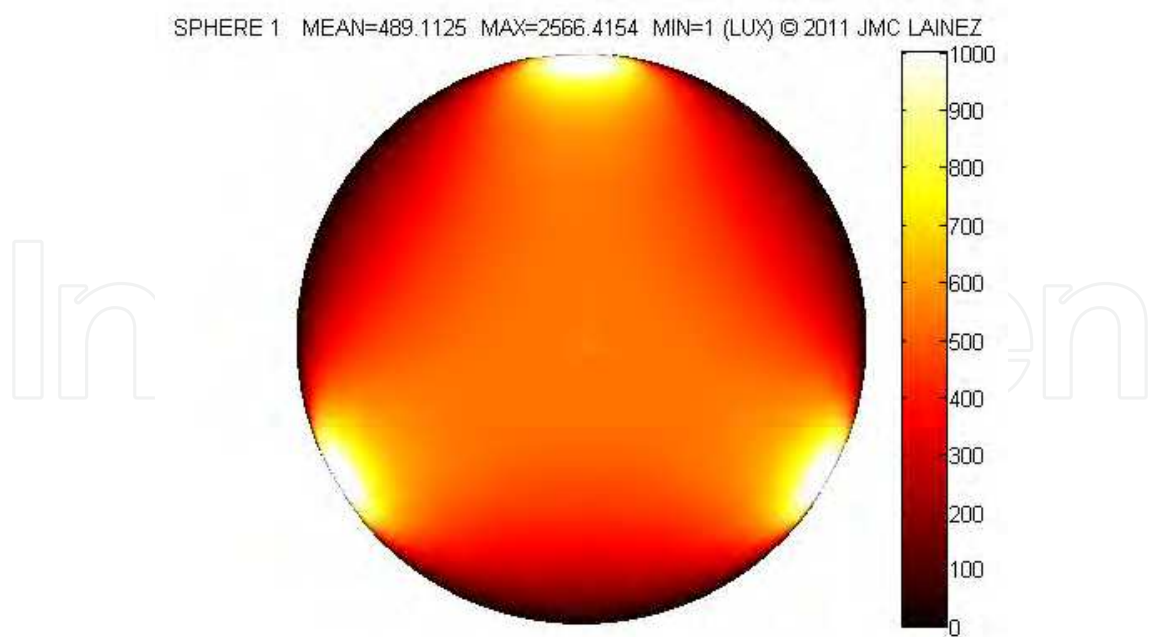


Fig. 9. Distribution of radiation on a sphere of radius 20 m. and reflectance 0.3, under three circular sources of 9 m. diameter and 10000 lumen/m<sup>2</sup> (lux) intensity, rotated 120°

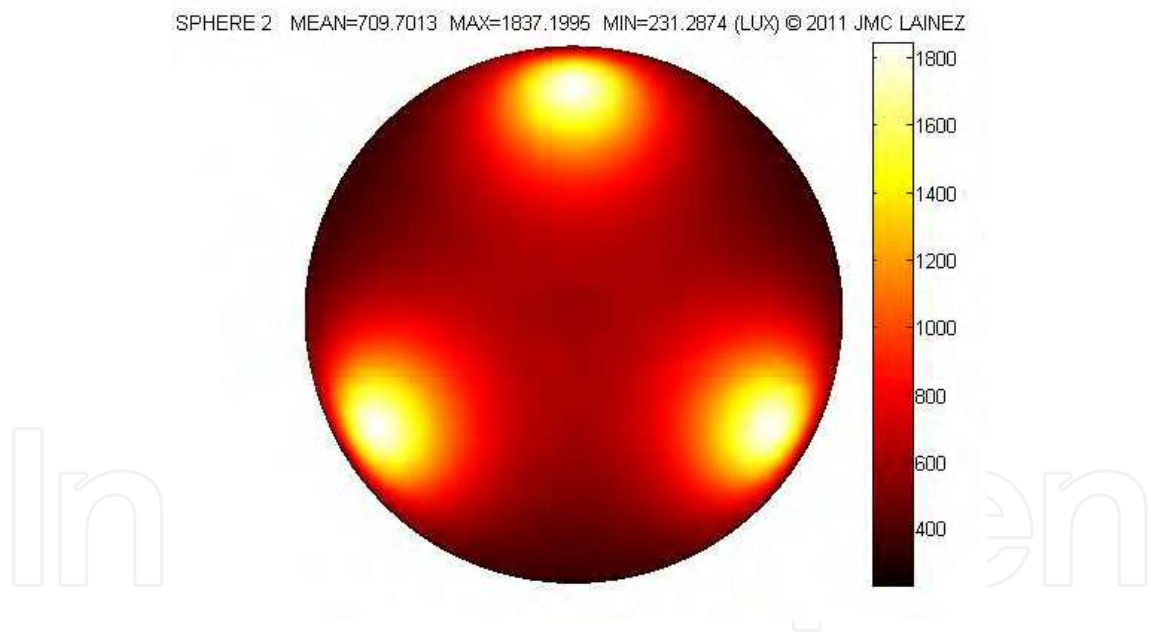


Fig. 10. The same three sources as in fig. 9 but radiation values are found instead on a circular disk 7.5 metres under the centre of the sphere

On the understanding that radiation fields are additive due to their vectorial nature, the author has solved with ease the fundamental problem of radiative transfer. To be sure, not all the openings<sup>2</sup> in buildings are circular but a significant amount of them can be approximated to one or several emitting disks with sufficient precision, taking into account

<sup>2</sup> The word “open” comes from ancient Greek οπή (opeh), meaning eye. The main aperture or vent in classic buildings is often termed “οπαιον” or “oculus”, its latin equivalent.

the inevitable lack of accuracy in the construction industry. In any case, the author has adapted his software to triangular and rectangular apertures (see section 4) but in the latter situation, solutions are not simple and require complex integration<sup>3</sup>.

2.2 Radiative transfer between complex surfaces

Once this matter is settled, retrieving the fundamental equation expounded at 8 to be partly solved in 10 and extending it to a second spherical cap as in figure 11, the radiant flux between the two caps of heights  $h_1$  and  $h_2$  is,

$$\phi_{1-2} = E_{b1} * \pi * h_1 * h_2 \tag{19}$$

For the area of the second cap is nothing but  $\pi * 2 * R * h_2$ .

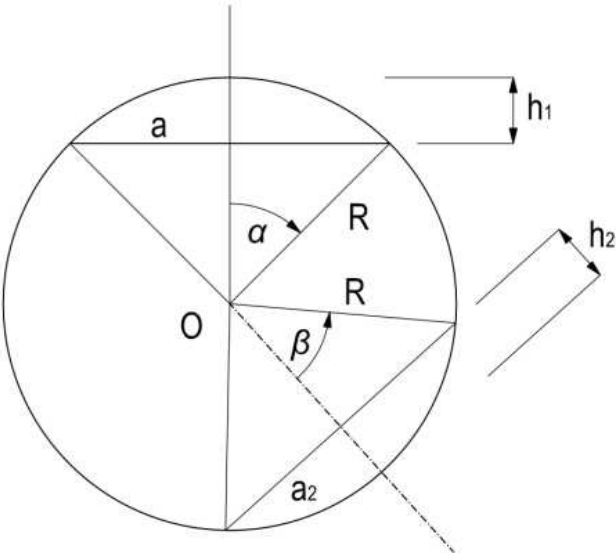


Fig. 11. Two spherical caps inside a sphere employed to find the radiative transfer

In the special situation that  $h_1 = h_2 = h$ , which often coincides with parallel disks of equal radius  $a$ , the flux would be  $E_{b1} * \pi * h^2$  and the fraction of energy from disk 1 to disk 2 (or their surrounding caps), equates  $h^2/a^2$ .

If only the perpendicular distance between the disks, called  $2b$ , is known (see figure 12), the height of the cap would be,

$$h = \sqrt{a^2 + b^2} - b \tag{20}$$

Thus, the fraction is obtained as,

$$F_{12} = F_{21} = \frac{a^2 + 2 * b^2 - 2 * b * \sqrt{a^2 + b^2}}{a^2} \tag{21}$$

<sup>3</sup> As a matter of fact only J. H. Lambert was capable of finding a solution for perpendicular rectangles with a common edge without the help of integration, but he often complained in his book of the “insurmountable difficulties” that the process entailed.

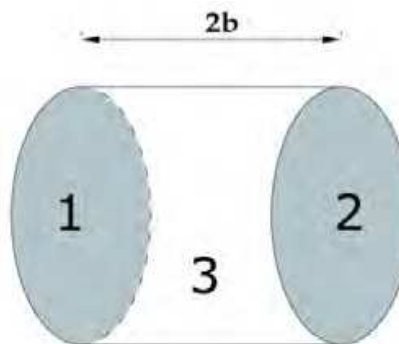


Fig. 12. Surfaces defined by a cylindrical volume used to find the radiative transfer

With the former expression, solving the radiative transfer inside cylinders is easy as there are only three surfaces involved and we can form a non-trivial system of two equations with two unknowns. Changing the circular base of the cylinder by a spherical cap (fig.13) will alter some values but not the general problem because all the possibilities of transfer between caps and disks have already been explored. For instance, if the cap is a hemisphere, the values of the factors to the disk and the cylinder need to be affected by  $a^2/(a^2 + h^2)=0.5$  (Eq. 4), and progressively until reaching one which is again the planar disk.<sup>4</sup>

The resulting volume in figure 13 has been used by humankind for centuries; mainly in churches but also in libraries, concert halls, banks, markets or pavilions of any sort. With another cap on the base, the form is more recently used for silos, fluid reservoirs and containment vessels at power stations.

Having solved the primary transference problems, the following step is the important subject of interreflections.

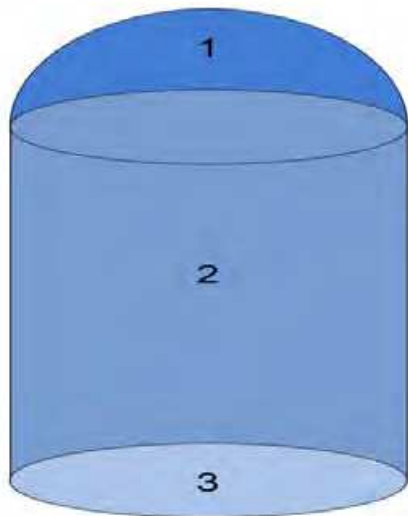


Fig. 13. Volume composed of a cylinder and a spherical cap used to find the radiative transfer among those surfaces

<sup>4</sup> Note that values under 0.5 can also be found for this relationship in a sort of globular cap with an area bigger than the hemisphere.

### 3. Interreflections among surfaces in a volume

Thus far, we have considered that energy is transferred from a primary source to several secondary ones. However this procedure does not deal with the fact that the receiving sources, being partially absorptive, may in turn become emitters.

In this situation, the total balance of energy is obtained by equation 22,

$$E_{tot} = E_{dir} + E_{ref} \quad (22)$$

Where  $E_{dir}$  represents the energy received directly and  $E_{ref}$  is the reflected energy. These two terms added give the total balance of radiative energy  $E_{tot}$ . When more than one surface is involved, expression 22 generates a system of equations. In order to solve it, it is useful to define *a priori* two similar matrices  $F_d$  and  $F_r$ , without physical entity, whose elements would be as follows, (for a volume contained by three surfaces like the one depicted in figure 13):

$$F_d = \begin{pmatrix} F_{11} * \rho_1 & F_{12} * \rho_2 & F_{13} * \rho_3 \\ F_{21} * \rho_1 & F_{22} * \rho_2 & F_{23} * \rho_3 \\ F_{31} * \rho_1 & F_{32} * \rho_2 & 0 \end{pmatrix} \quad (23)$$

$$F_r = \begin{pmatrix} 1 & -F_{12} * \rho_2 & -F_{13} * \rho_3 \\ -F_{21} * \rho_1 & 1 & -F_{23} * \rho_3 \\ -F_{31} * \rho_1 & -F_{32} * \rho_2 & 1 \end{pmatrix} \quad (24)$$

Where  $F_{ij}$  are the radiative exchange fractions or factors from surface  $i$  to surface  $j$  found previously, and  $\rho_i$  is a new term, defined as the coefficient of diffuse or direct reflection which can be attributed to surface  $i$ . It can be obtained as the quotient between the energy received and the energy effectively emitted.

This is the reason why in matrix  $F_d$  described at 23, the element in column 3, row 3, is zero as a planar disk does not send radiation to itself.

However, if we should have a curved surface it would be necessary to substitute the former element by  $F_{33} * \rho_3$ . On the contrary, in a volume defined by planes, all the elements in the diagonal of matrix  $F_d$  are equal to zero.

Once the value of these matrices is obtained, it is easy to establish a relationship between direct and reflected radiation:

$$F_r * E_{ref} = F_d * E_{dir} \quad (25)$$

$$F_{rd} = F_r^{-1} * F_d \quad (26)$$

$$E_{ref} = F_{rd} * E_{dir} \quad (27)$$

As the value of reflected radiation is known, the problem is solved. However, we have to bear in mind that the minimum of surfaces in an actual room would be six.

Recently, the author has developed software for up to twelve surfaces inside a room. This will augment precision at the cost of a lengthier input of data.

The process of interreflection can be repeated many times until no significant changes in reflected radiation are observed.

Again, a simple case of this reiterative process occurs in the sphere and is often used as a substitute for the calculations described.

In equation 10 and successive, it was stated that the energy received by a point in the sphere from any surface contained in the same sphere was equivalent to the ratio between the area of the emitting surface and the total area  $4\pi R^2$ , this can be written  $W/A$ .

After infinite rebounds, the energy reflected on the sphere would be:

$$E_{ref} = E * \frac{W}{A} * (\rho + \rho^2 + \dots \rho^n) \quad (28)$$

As,

$$\lim_{n \rightarrow \infty} \left( \frac{\rho^{n+1}-1}{\rho-1} - 1 \right) = \frac{\rho}{1-\rho} \quad (29)$$

$$E_{ref} = E * \frac{W}{A} * \left( \frac{\rho}{1-\rho} \right) \quad (30)$$

$\rho$  in the former equations means the average of the reflection coefficients  $\rho_i$  and  $E$  is the direct energy emitted by the source. Therefore, this equation is suitable for all kinds of volumes, but its accuracy diminishes as the actual room is dissimilar to a sphere. Under these circumstances, equation 27 is preferable to equation 30.

As the reflectance of the room surfaces may be shifted at will, it is possible to conceive some of great absorptiveness which can be equated to virtual or transparent surfaces and, in that manner we would deal with semi-open spaces or non-reflecting elements. For instance, the former enables us to address the urban canyon and consequently the radiative transfer that takes place in urban spaces. To perform that kind of analysis, the energy exchanges in parallelepipeds must be obtained in advance.

#### 4. Radiative transfer between plane surfaces

There is no special problem in extending what we had found for the vertical component of the disk in equation 15 and the corresponding section. Only a cartesian reticule instead of polar is needed.

This new equation, albeit not difficult, especially for the computer, is greatly altered, when compared with the simple  $h/2R$ .

$$f(x, y) = \frac{E}{2} \left[ 1 - \frac{x^2 + y^2 + z^2 - a^2}{\sqrt{(x^2 + y^2)^2 + 2*(x^2 + y^2)*(z^2 - a^2) + (z^2 + a^2)^2}} \right] \quad (31)$$

In expression 31,  $z$  is the vertical distance to the point considered on the graticule and  $a$ , is the radius of the source as before. The resulting field for the horizontal direction can be seen in figure 14.

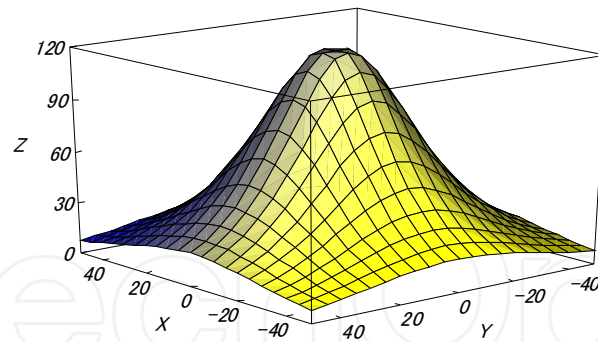


Fig. 14. Radiative field on a horizontal cartesian surface due to a disk source

If the disk turns to a rectangle, then the factor that gives the energy fractions, shows an entirely different configuration,

$$f(x, y) = \frac{E}{2} \left[ \frac{y}{\sqrt{z_2^2 + y}} \left( \arctan \frac{x + \frac{a}{2}}{\sqrt{z_2^2 + y}} - \arctan \frac{x - \frac{a}{2}}{\sqrt{z_2^2 + y}} \right) - \frac{y}{\sqrt{z_1^2 + y}} \left( \arctan \frac{x + \frac{a}{2}}{\sqrt{z_1^2 + y}} - \arctan \frac{x - \frac{a}{2}}{\sqrt{z_1^2 + y}} \right) \right] \quad (32)$$

Where  $a$ , is the width of the rectangle and the height is  $z_2 - z_1$ .

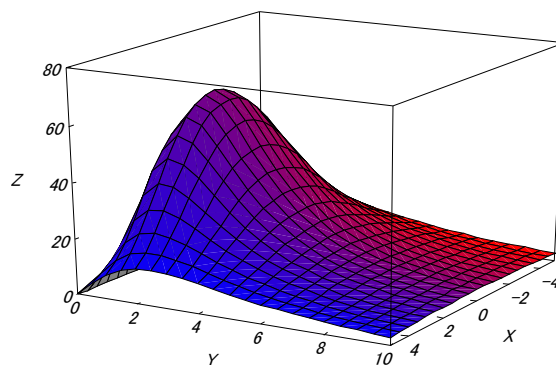


Fig. 15. Radiative field on a horizontal cartesian surface due to a vertical rectangular emitter

As in the case of the circular source, the horizontal component of the radiation vector has a more complex formulation. The reader may find further information in the references given. Without this component and a third perpendicular one, because now the analysis is performed in cartesian space instead of spherical, the vector remains undefined. This may lead to considerable inexactitude.

Turning to the exchange between surfaces as a whole, the mathematical procedure is indeed cumbersome and exceeds the scope of this chapter, though the author has been capable of completing it (see references). In order to program the solution for the computer in a more efficient way, it is often convenient to follow the method proposed by Yamauchi<sup>5</sup> (Yamauchi, 1934).

<sup>5</sup> Paradoxically, this clever procedure was invented to overcome the lack of computational capacities.



In this procedure the value of function  $\Phi$ , is found for a different set of angles related with the dimensions of the surfaces considered.

$$\phi_0(\mu) = \frac{1}{2} * (\mu - \frac{1}{2} * \tan(\mu) * \ln(\sin(\mu))) + \frac{1}{2} * \cotan(\mu) * \ln(\cos(\mu)))$$

(33)

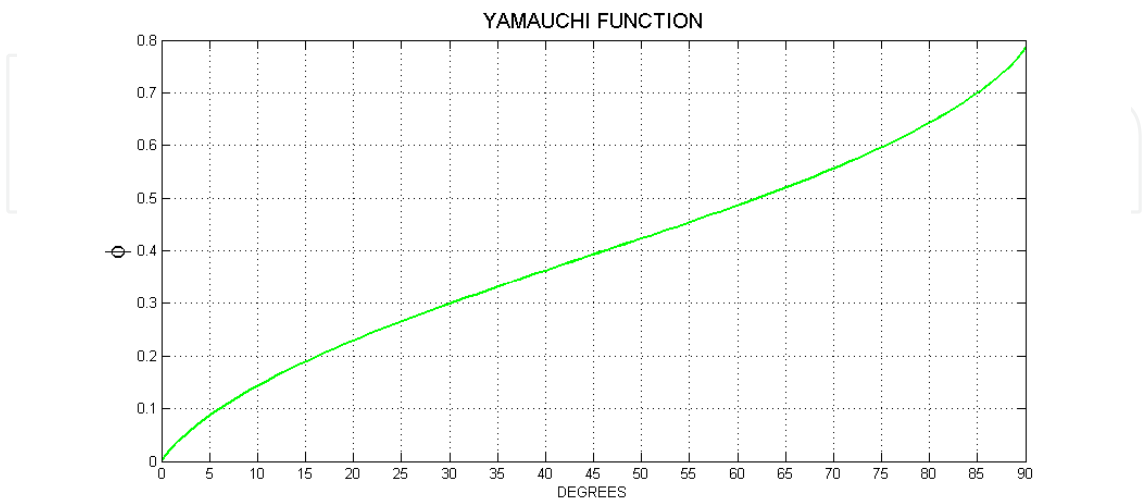


Fig. 16. Graph of the Yamauchi function from 0 to 90 degrees

The set of angles previously mentioned is obtained by looking at figure 17 and equations 34 to 36.

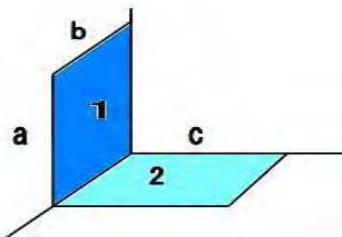


Fig. 17. Perpendicular surfaces with a common edge used to find the energy transfer

$$\alpha = \arctan(b/a)$$

(34)

$$\beta = \arctan(b/c)$$

(35)

$$\beta_1 = \arctan\left(\frac{b}{\sqrt{a^2+c^2}}\right)$$

(36)

Thus, the fraction of energy from surface 1 to surface 2 is,

$$F_{12} = \frac{2}{a*\pi} \left[ a * \phi_0(\alpha) + c * \phi_0(\beta) - \sqrt{a^2 + c^2} * \phi_0(\beta_1) \right]$$

(37)

5. Radiative transfer in a space composed of several volumes

A further step that the author has devised consists of subdividing a complex space in several simpler volumes whose performance is eventually concatenated. The author has called this procedure the Superposition Principle of Radiation.



This situation is convenient for the treatment of several building features that perform as radiation filters such as canopies, awnings, louvers and even courtyards or reflective ponds.

For instance, in a system of louvers it is possible to isolate the volume seen in figure 18 and treat it as a single space with three virtual faces. Once the radiation that reaches the surface of the glass is obtained, the procedure is the same as for a room without louvers but the emissive power used for the window is the previous value and not the one applicable for the unobstructed orientation.

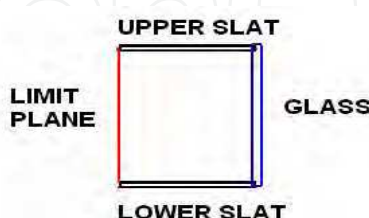


Fig. 18. Subdivision of louvers in a protected window

In this way, most of the problems derived from the geometry of the design are solved and radiation filters can be properly evaluated. Previously they were only considered obstructions without any potential to add for the energy balance.

## 6. Discussion and simulation examples

With all that we have expounded thus far, the reader is in the position to extract useful consequences to find the performance of radiation in buildings, either existing or projected.

Using his original software, based on the former section, the author has conducted a wide variety of simulations around the world. Most of them were validated by means of direct monitoring, both automatic and manual where available.

However, some provisos have to be taken into account. First of all, it has been assumed that radiation is emitted in a diffuse manner following Lambert's law. While this may be true for many materials especially modern ones, when dealing with heritage buildings such properties may not be accurate. In fact, the reflectance of surfaces at no longer extant architectural spaces remains largely unknown.

Even more difficult is the question of glazing in ancient buildings. Transparent glass panes which follow quantum dynamics in transmitting radiation are relatively modern. An added constraint is the fact that, recently, a wide variety of systems capable of selective or holographic transmission has been made accessible to designers and builders.

The main solution has been to define a directional or volumetric transmittance for glazing. This is a similar concept to the well-known photometric curve and gives us the spatial or spectral properties of glass-emitters. For the time being, these transformations can only admit bi-ellipsoidal form in the author's software.

For these and other reasons, interferences of radiation like diffraction and scattering, though predictable, are not handled in their entirety. Fortunately these phenomena are not very common in the building industry, especially because they may lead to visual discomfort and are generally avoided by users and designers.

Once the radiative transfer is settled for a given space through its geometric and optic features, the amount of renewable energy available is known. This may become an important figure in the energy analysis or may have a thermal or visual correlate. The visual results are more intuitive than the thermal ones.

To find the temperature field due to radiation on a surface, Stefan-Boltzmann's law has to be invoked and significant differences with the luminous domain emerge. The first and more relevant one is that the temperature of the surfaces considered has to be found or estimated since there are no elements at 0 K in buildings. The author's and other correlations help in this respect but may not be definitive. A second proviso is that reflectances for thermal radiation are not similar to those in the luminous domain. Fortunately, most of them fall into the range of 0.9 for interior building surfaces.

Finally, if due to ventilation a convective field coincides with that provided by radiation, the latter, according to our experiments, will not be significantly altered in the short term because what is mostly affected is the thermal sensation.

With all the former in mind, the author would like to present the simulation cases of two paradigms of ancient Roman architecture, whose accurate radiative performance was largely unknown: the Pantheon and its superb baroque evolution the Church of Sant'Andrea all Quirinale. The architect and sculptor of light Gian Lorenzo Bernini completed this masterpiece, considered to be his own spiritual retreat.

Following the discussion of radiation in centralised spaces, a building currently under construction, the new railway station at the airport of Barcelona (Spain) is briefly presented in an effort to show how simulation can help in the design process and assessment.

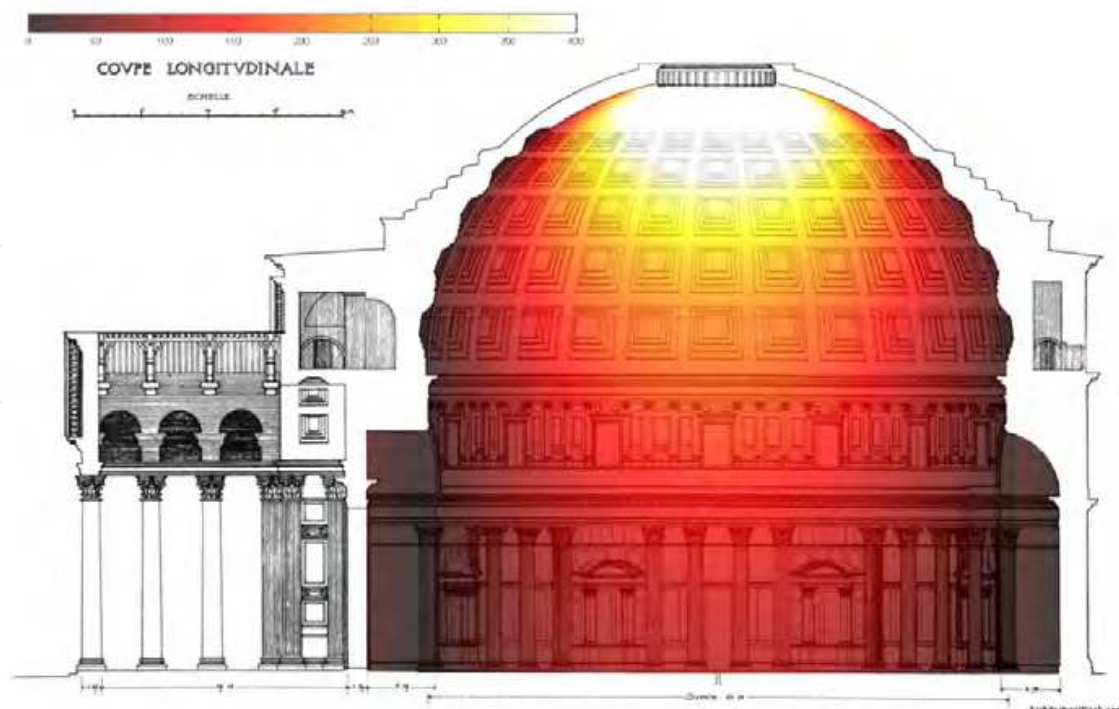


Fig. 19. The Roman Pantheon illuminated by diffuse radiation of an intensity of 10000 lumen/m<sup>2</sup> (lux). A typical situation in autumn and spring. Scale 0 to 400 lux

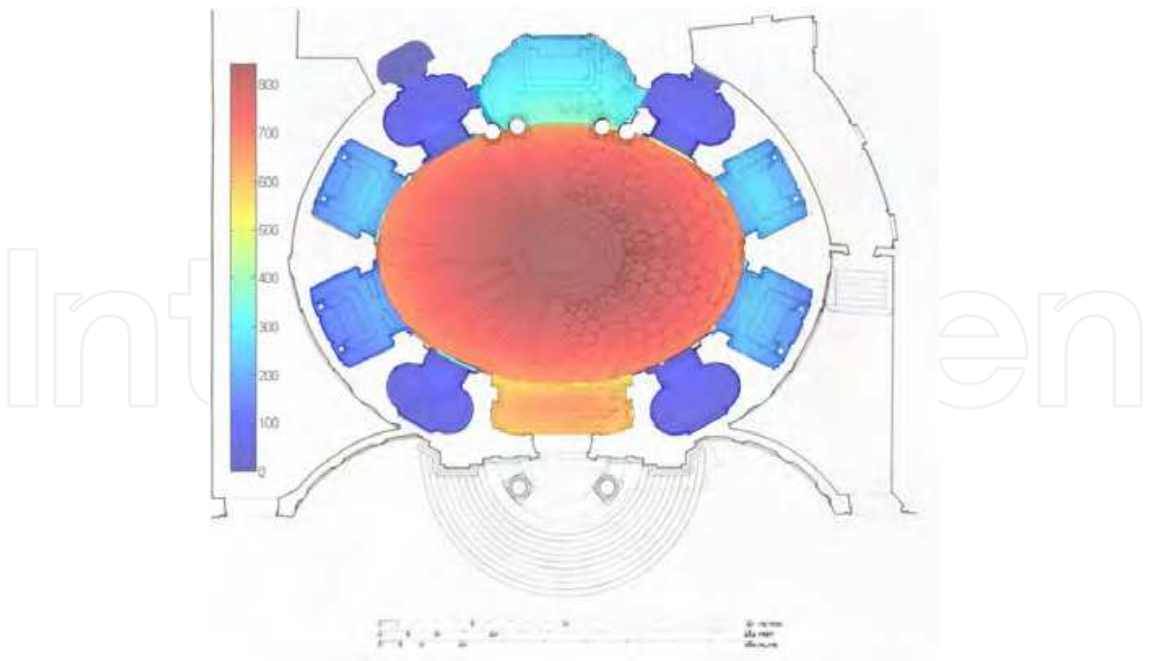


Fig. 20. Sant'Andrea all Quirinale's Church by Bernini (Rome) illuminated by direct solar radiation in winter. Values in lux(0-800)

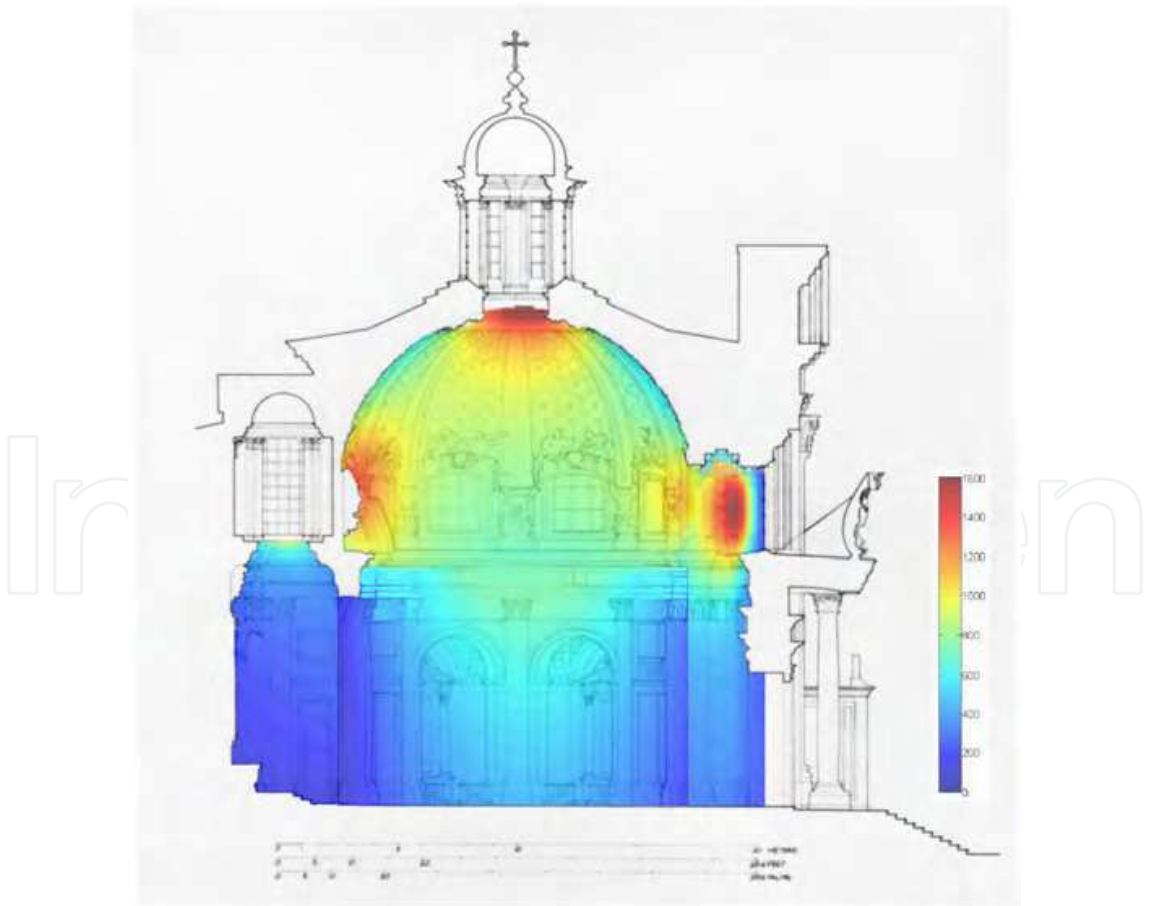


Fig. 21. Sant'Andrea all Quirinale's Church. Section under direct solar radiation in winter. Values in lux(0-1600)

The final case to be introduced is the Rautatalo building of 1955, by the modern Finnish master Alvar Aalto. Originally a department store, it beckoned Helsinki’s citizens by its intelligent use of luminous radiation, enhanced by conical skylights subtly adapted to the solar path in this northern city.

In the first two examples, luminous radiation is nuanced and constant for the lower spaces. It is outlined that the values for the Pantheon were not significant (sometimes, under 200 lux) and this fact may have led to the introduction of vertical windows in the drum of the cylinder by late Renaissance or Baroque epochs. Radiative performance does not show an acute seasonal variation, but allows for sunshine to reveal certain decorative details of the structure adding to the reputation of spiritual luminous atmosphere that encompass the work of Bernini. A hall of more than 300 square metres featuring a consistent level of 800 lux with only nine carved windows and the magnificent lantern is remarkable for the 17<sup>th</sup> century.

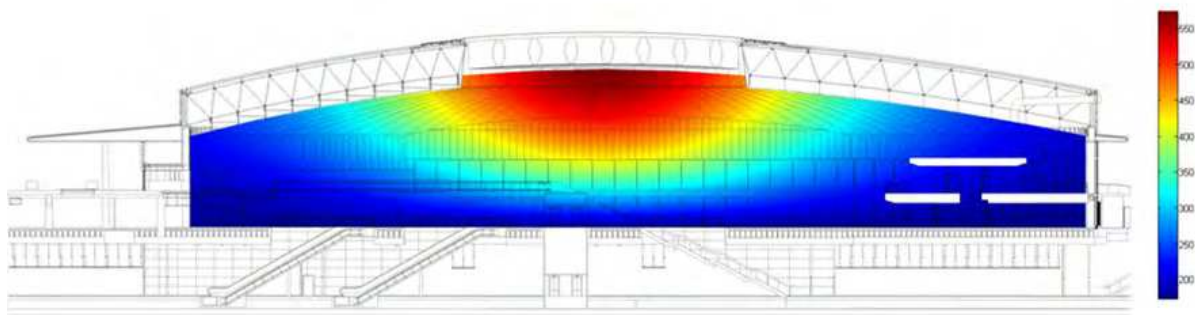


Fig. 22. Section of the new railway station in Barcelona. Radiation design by the author. Project by the architects Cesar Portela and Antonio Barrionuevo. Values in lux (0-600)

Changing the scale for the modern requirements of transportation spaces which have become the cathedrals of our time, the author proposes a lighting design in which the oculus reaches a diameter of 35 metres and the radiative energy is distributed by means of massive aluminium louvers with a height exceeding 3 metres in total. The simulation shows good levels and an acceptable raise of temperature at the glazed aperture due to the mild climate of Barcelona.

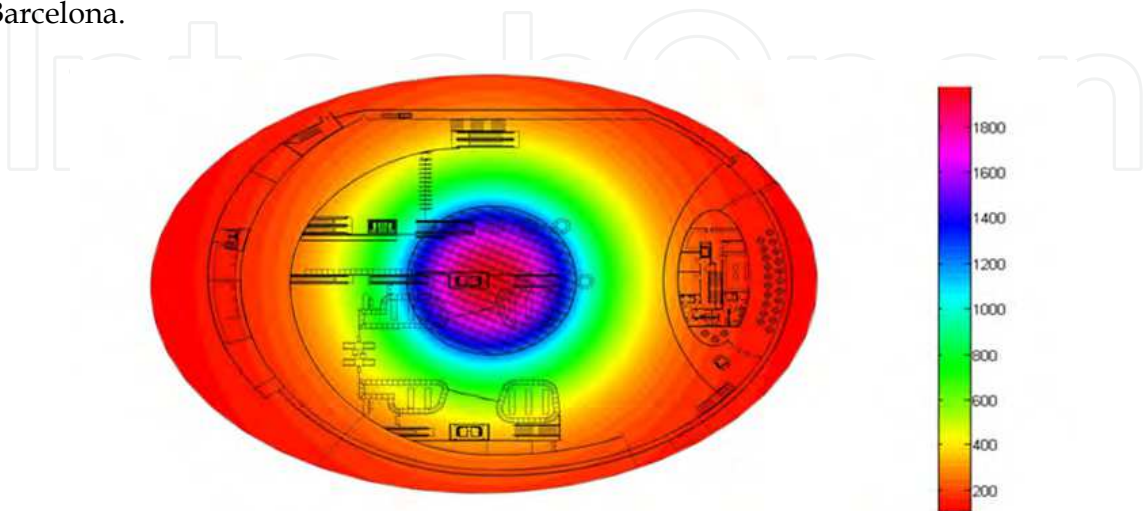


Fig. 23. Plan of the railway station in summer. Values in lux



The last example, the Rautatalo building, brings the reader back to the efforts of the modern movement in architecture to control radiation. With 40 skylights it was subsequently adapted to many projects around the world, which generally speaking fared less well than the original for climatic and economic circumstances.

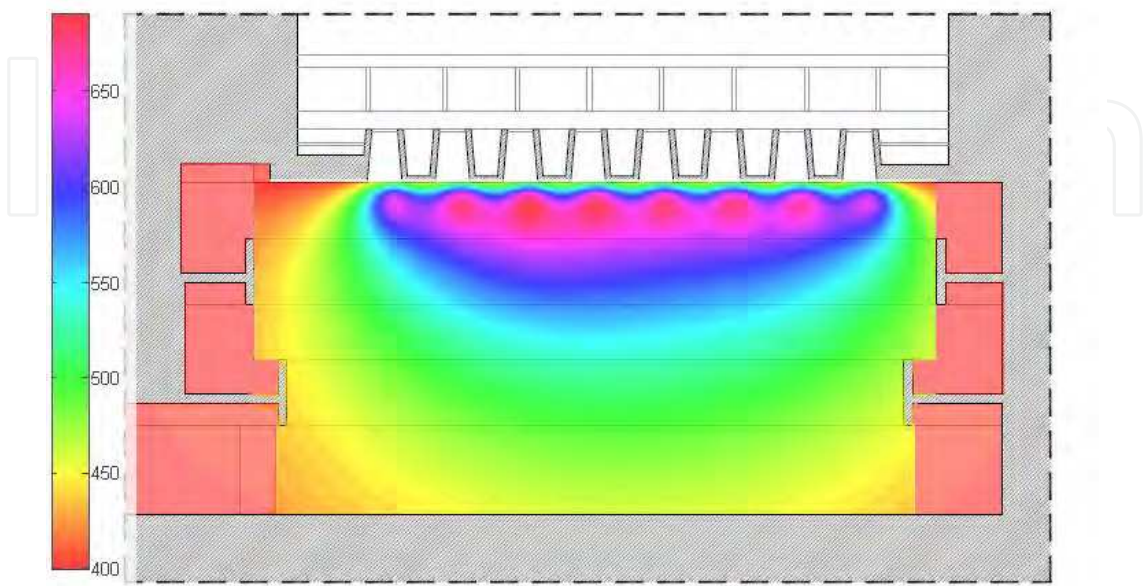


Fig. 24. The Rautatalo building of 1955 by Alvar Aalto, Helsinki. Simulation of 40 skylights (8\*5), performed in June with direct sunlight and monitored on 21<sup>st</sup> of June 2011. Values in lux

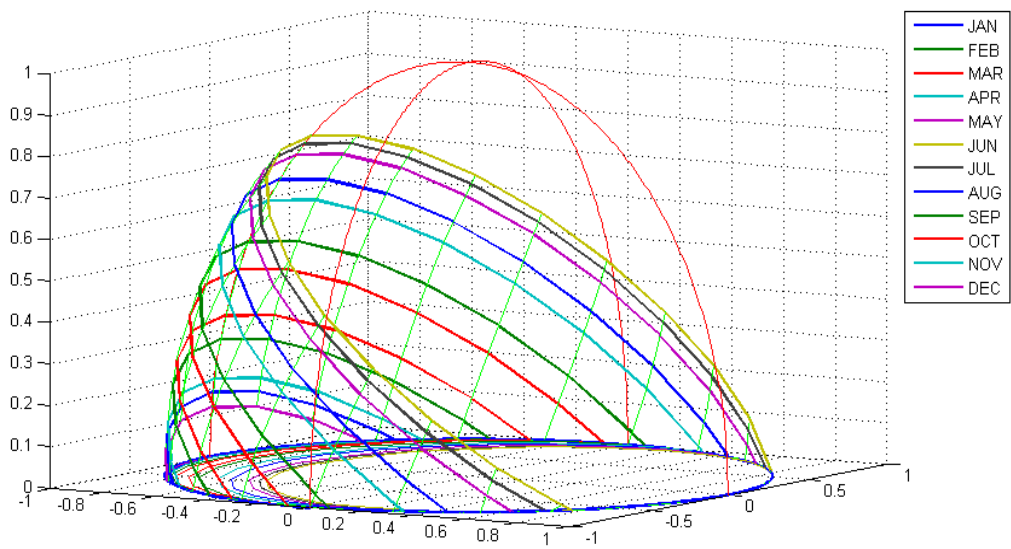


Fig. 25. Solar Chart of Helsinki. Latitude 61.16 degrees north

This climate-responsive building would remind the reader that, in order to produce universal results there is the need to consider local weather parameters.

7. Weather data

As figure 25 tries to evoke, weather data for radiation must be based on sunlight availability. At the time of writing this chapter, many measurements of horizontal irradiation in the world have been recorded and also correlations for vertical surfaces of different orientations are available. The author recommends the following based on altitude  $\theta$  and azimuth  $\varphi$  from the south direction (in radians).

$$E_v = 4000 * \theta^{1.3} + 12000 * \sin^{0.3} \theta * \cos^{1.3} \theta * [(2 + \cos \varphi) / (3 - \cos \varphi)]$$

(38)

The author’s software is capable of combining these results with sunlight probability for any location in the world to obtain annual, monthly and hourly distribution of irradiance on vertical and horizontal surfaces. (See tables 1 and 2).

	NORTH	EAST	SOUTH	WEST	HORIZONTAL
DIFFUSE	46,57	67,04	85,19	67,04	113.79
DIRECT	39,40	283,89	271.16	283,89	290.31
GLOBAL	85,97	350,93	356.35	350,93	404.11

Table 1. Mean annual radiation (W/m²) by orientation in Rome. Italy.  
Latitude= 43.41° North

	SOUTH	EAST	NORTH	WEST	HORIZONTAL
DIFFUSE	72,56	81,02	77,41	81,02	152,44
DIRECT	147,85	348,94	173,78	348,94	428,05
GLOBAL	220,42	429,96	251,19	429,96	580,49

Table 2. Mean annual radiation (W/m²) by orientation in Quito. Ecuador.  
Latitude= 0.3° South

Nonetheless, the former data are averages and not a substitute for measured registers and much less for instant values. Only simultaneous monitoring at intelligent buildings can achieve real time input in our simulation model.

What is recommended in this chapter is a likely figure intended to handle the problem with reasonable accuracy in the frequent absence of more detailed information. This will help to design building features that save energy and comply with the most relevant weather conditions at each climate<sup>6</sup>.

<sup>6</sup> Klymax κλίμαξ in Greek from where the word climate derives, means “stairway”.

## 8. Conclusion

The author has produced some innovative tools which prove to be highly efficient and compatible with those currently employed in architectural and engineering projects. In doing so, it is his firm belief that creativity and freedom of design in the realm of solar radiation will be much enhanced. The so-created software is universal and it aims to bridge the gap in solar design between developed and non-developed regions.

The conscious application of these techniques also brings new possibilities to benefit from solar radiation in our own homes. This is in the author's hope, a good way to help the peoples in the world, in a moment of turbulence and social unrest.

The main drawback found is the lack of preparedness of many architects and authorities to implement these methods in the decision-making process.

With the warp thus created fabrics can be woven as usual, although it is also possible to make a sort of net out of it and lie down at ease, or perchance play with it as a makeshift harp and see how it sounds! For as Coleridge once wrote<sup>7</sup>,

And what if all of animated nature

Be but organic Harps diversely fram'd

That tremble into thought

## 9. Acknowledgment

The author wants to recognize the help of the following people: Miss Patricia Karlsson of the National Pension Institution of Helsinki, who was instrumental in revealing Aalto's mastery of light; the kindness and assistance of Professor Mojita Navvab of the University of Michigan are deeply appreciated. Among many other favours, he granted access to MacAllister's original papers. Karma, my research group of the University of Seville was extremely supportive, especially Professors Jesus Pulido and Viggo Castilla; and in Japan, Professor Tetsushi Okumura of the University of Nagoya has always been helpful.

Finally, it is the author's wish to praise the Japanese people for their tenacity and profound respect of Nature, regardless of the tragic blows that She may inflict on this beloved land.

## 10. References

- Ashdown I. (2004). *Radiosity: A Programmer's Perspective*. John Wiley & Sons Inc. New York, 1994. Available from <http://www.helios32.com>.
- Baker, N. V., Fanchiotti, A., Steemers, K. N. (1993). *Daylighting in Architecture. A European Reference Book*. Commission of the European Communities. Directorate General XII.

---

<sup>7</sup> Samuel T. Coleridge. *The Aeolian Harp*. 1795

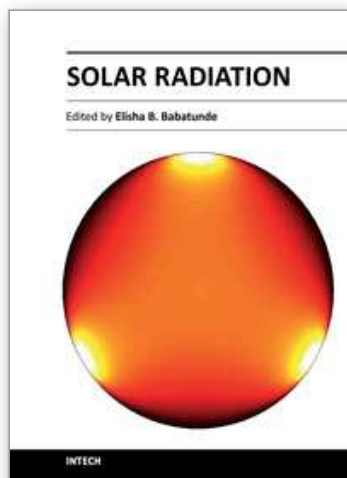
- Cabeza Lainez, J.M. (2010). *Fundamentos de Transferencia Radiante Luminosa*. (Including software for simulation). Netbiblo. Spain.
- Cabeza Lainez, J.M. (1999). Scientific designs of sky-lights. *Conference on passive and low energy architecture* (PLEA). Brisbane. Australia.
- Cabeza Lainez, J. M. (2007). The Japanese experience of environmental architecture through the works of Bruno Taut and Antonin Raymond. Vol.6 I. Pgs. 33-40. *Journal of Asian Architecture and Building Engineering* (JAABE). ISSN: 1346-7581
- Cabeza Lainez, J. M. (2007). Radiative performance of louvres, Simulation and examples in Asian Architecture. *IAQVEC*. Volume III . ISBN: 978-4-86163-072-9 C3052 \4762E. Sendai (Japan).
- Cabeza Lainez, J. M. (2008). The Quest for Light in Indian Architectural Heritage. Vol.7 I. Pgs. 17-25. *Journal of Asian Architecture and Building Engineering* (JAABE). ISSN: 1346-7581.
- Cabeza Lainez, J.M. (2009) *Lighting Features in Japanese Traditional Architecture*. In "Lessons from Traditional Architecture". Editors, Yannas, S., Weber, W. Earthscan. London. ISBN 9781844076000
- DiLaura D. L. (1999). New procedures for Calculating Diffuse and Non-Diffuse Radiative Exchange Form Factors. *Proceedings of ASME*.
- Feynman, R. P. (1990). *Quantum electrodynamics: The Strange Theory of Light and Matter*. Penguin Books.
- Fock, V. (1924). *Zur Berechnung der Beleuchtungsstärke*. Optisches Institut St. Petersburg.
- Garibaldi, C. (1994). *Simulazione deterministica della radiazione solare nella chiesa di San Lorenzo a Torino*. CNR Italy.
- Higbie, H. H. (1934) *Lighting Calculations*. John Wiley and Sons. New York.
- Holman, J.P. (1997) *Heat Transfer*. Mac Graw-Hill. New York.
- Hopkinson, R. G.; Petherbridge, P.; Longmore, J. (1966) *Daylighting*. London. Heinemann.
- Kimura, K. (1977). *Scientific Basis of Air Conditioning*. Amsterdam. Elsevier.
- Lambert J. H. (1764). *Photometria. sive de mensura et gradibus Luminis, Colorum et Umbrae*. Editor. D. DiLaura. IESNA. 2001.
- MacAllister, A. S. (1910). Graphical Solutions of Problems Involving Plane-Surface Lighting Sources . *Lighting World* 56. No.1356.
- Moon, P. H; Spencer D. E. (1981) *The Photoc Field*. The MIT Press. Cambridge. Massachusetts.
- Moon, P. H. (1962) *The Scientific Basis of Illuminating Engineering*. Dover Publications. New York.
- Moore, F. (1991). *Concepts and Practice of Architectural Daylighting*. Van Nostrand Reinhold. New York.
- Ne'eman, E. (1974) Visual Aspects of Sunlight in Buildings. *Lighting Research and Technology*. Vol 6. N° 3.
- Pierpoint, W. (1983). A Simple Sky Model for Daylighting Calculations. *International Daylighting Conference*. Phoenix.
- Robbins, C. L. (1986). *Daylighting. Design and Analysis*. Van Nostrand Reinhold. New York.
- Shukuya M, (1993) *Hikari to Netsu no Kenchiku Kankyôgaku* -Light and temperature in Environmental Science - (in Japanese). Maruzen. Tokyo.



- Yamauchi, J. (1927). The Light Flux Distribution of a System of Inter-reflecting Surfaces. *Researches of the Electro-technical Laboratory*. No. 190. Tokyo. (In Japanese).
- Yamauchi, J. (1929). The Amount of Flux Incident to Rectangular Floor through Rectangular Windows. *Researches of the Electro-technical Laboratory*. No. 250. Tokyo.
- Yamauchi, J. (1932). Theory of Field of Illumination. *Researches of the Electro-technical Laboratory*. Tokyo. No. 339.

IntechOpen

IntechOpen



### **Solar Radiation**

Edited by Prof. Elisha B. Babatunde

ISBN 978-953-51-0384-4

Hard cover, 484 pages

**Publisher** InTech

**Published online** 21, March, 2012

**Published in print edition** March, 2012

The book contains fundamentals of solar radiation, its ecological impacts, applications, especially in agriculture, architecture, thermal and electric energy. Chapters are written by numerous experienced scientists in the field from various parts of the world. Apart from chapter one which is the introductory chapter of the book, that gives a general topic insight of the book, there are 24 more chapters that cover various fields of solar radiation. These fields include: Measurements and Analysis of Solar Radiation, Agricultural Application / Bio-effect, Architectural Application, Electricity Generation Application and Thermal Energy Application. This book aims to provide a clear scientific insight on Solar Radiation to scientist and students.

### **How to reference**

In order to correctly reference this scholarly work, feel free to copy and paste the following:

Jose Maria Cabeza Lainez (2012). Solar Radiation in Buildings, Transfer and Simulation Procedures, Solar Radiation, Prof. Elisha B. Babatunde (Ed.), ISBN: 978-953-51-0384-4, InTech, Available from: <http://www.intechopen.com/books/solar-radiation/solar-radiation-in-buildings-transfer-and-simulation-procedures>

**INTECH**  
open science | open minds

### **InTech Europe**

University Campus STeP Ri  
Slavka Krautzeka 83/A  
51000 Rijeka, Croatia  
Phone: +385 (51) 770 447  
Fax: +385 (51) 686 166  
[www.intechopen.com](http://www.intechopen.com)

### **InTech China**

Unit 405, Office Block, Hotel Equatorial Shanghai  
No.65, Yan An Road (West), Shanghai, 200040, China  
中国上海市延安西路65号上海国际贵都大饭店办公楼405单元  
Phone: +86-21-62489820  
Fax: +86-21-62489821

© 2012 The Author(s). Licensee IntechOpen. This is an open access article distributed under the terms of the [Creative Commons Attribution 3.0 License](https://creativecommons.org/licenses/by/3.0/), which permits unrestricted use, distribution, and reproduction in any medium, provided the original work is properly cited.

IntechOpen

IntechOpen